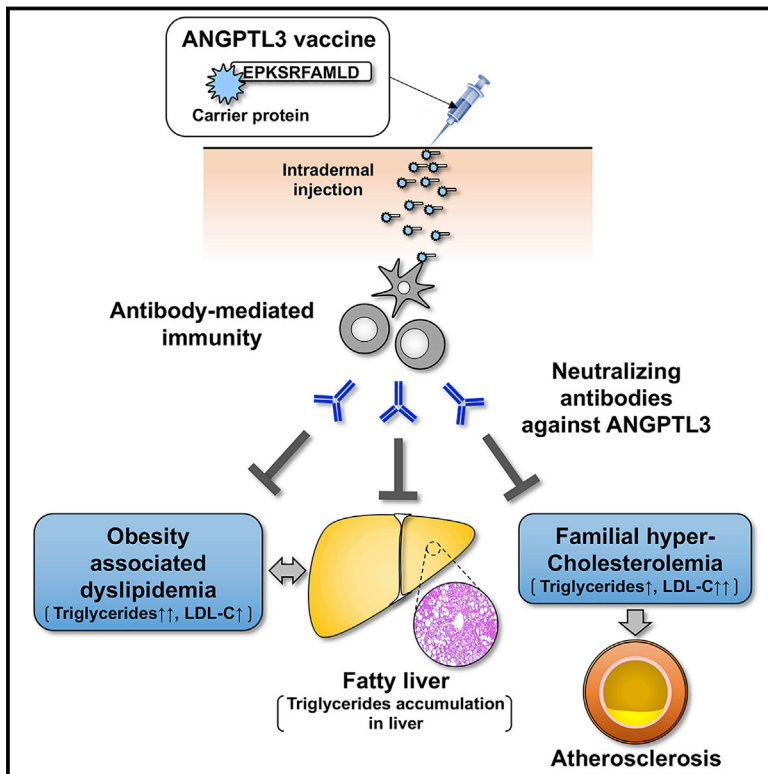


# Vaccine targeting ANGPTL3 ameliorates dyslipidemia and associated diseases in mouse models of obese dyslipidemia and familial hypercholesterolemia

## Graphical Abstract



## Authors

Hiroataka Fukami, Jun Morinaga, Hironori Nakagami, ..., Masashi Mukoyama, Ryuichi Morishita, Yuichi Oike

## Correspondence

oike@gpo.kumamoto-u.ac.jp

## In brief

Fukami et al. demonstrate that immunization with a peptide vaccine targeting ANGPTL3 improves dyslipidemia and fatty liver in B6.Cg-*Lep<sup>ob</sup>/J* (*ob/ob*) mice. ANGPTL3 vaccine also improves dyslipidemia and atherosclerosis development in B6.KOR/*StmSlc-Apoe<sup>shl</sup>* mice fed a high-cholesterol diet, which represent a model of severe familial hypercholesterolemia caused by ApoE loss of function.

## Highlights

- We generate a peptide vaccine targeting ANGPTL3 with a durability of ~30 weeks
- ANGPTL3 vaccine improves obesity-induced dyslipidemia and fatty liver in mice
- The vaccine improves dyslipidemia in familial hypercholesterolemia model mice
- The vaccine improves atherosclerosis in familial hypercholesterolemia model mice



## Article

# Vaccine targeting ANGPTL3 ameliorates dyslipidemia and associated diseases in mouse models of obese dyslipidemia and familial hypercholesterolemia

Hirota Fukami,<sup>1,2,3,7</sup> Jun Morinaga,<sup>1,2,3,7</sup> Hironori Nakagami,<sup>4</sup> Hiroki Hayashi,<sup>4</sup> Yusuke Okadome,<sup>1</sup> Eiji Matsunaga,<sup>1,2</sup> Tsuyoshi Kadomatsu,<sup>1,3</sup> Haruki Horiguchi,<sup>1,3,5</sup> Michio Sato,<sup>1,3</sup> Taichi Sugizaki,<sup>1,3</sup> Takashige Kuwabara,<sup>2</sup> Keishi Miyata,<sup>1,3</sup> Masashi Mukoyama,<sup>2</sup> Ryuichi Morishita,<sup>6</sup> and Yuichi Oike<sup>1,3,5,8,\*</sup>

<sup>1</sup>Department of Molecular Genetics, Graduate School of Medical Sciences, Kumamoto University, 1-1-1 Honjo, Chuo-ku, Kumamoto 860-0556, Japan

<sup>2</sup>Department of Nephrology, Graduate School of Medical Sciences, Kumamoto University, 1-1-1 Honjo, Chuo-ku, Kumamoto 860-0556, Japan

<sup>3</sup>Center for Metabolic Regulation of Healthy Aging (CMHA), Graduate School of Medical Sciences, Kumamoto University, 1-1-1 Honjo, Chuo-ku, Kumamoto 860-0556, Japan

<sup>4</sup>Department of Health Development and Medicine, Osaka University Graduate School of Medicine, 2-2, Yamadaoka, Suita, Osaka 565-0871, Japan

<sup>5</sup>Department of Aging and Geriatric Medicine, Graduate School of Medical Sciences, Kumamoto University, 1-1-1 Honjo, Chuo-ku, Kumamoto 860-0556, Japan

<sup>6</sup>Department of Clinical Gene Therapy, Osaka University Graduate School of Medicine, 2-2, Yamadaoka, Suita, Osaka 565-0871, Japan

<sup>7</sup>These authors contributed equally

<sup>8</sup>Lead contact

\*Correspondence: [oike@gpo.kumamoto-u.ac.jp](mailto:oike@gpo.kumamoto-u.ac.jp)  
<https://doi.org/10.1016/j.xcrm.2021.100446>

## SUMMARY

Dyslipidemia is a risk factor for cardiovascular disease (CVD), a major cause of death worldwide. Angiotensin-like protein 3 (ANGPTL3), recognized as a new therapeutic target for dyslipidemia, regulates the metabolism of low-density lipoprotein-cholesterol (LDL-C) and triglycerides. Here, we design 3 epitopes (E1–E3) for use in development of a peptide vaccine targeting ANGPTL3 and estimate effects of each on obesity-associated dyslipidemia in B6.Cg-*Lep<sup>ob</sup>/J (ob/ob)* mice. Vaccination with the E3 (<sup>32</sup>EPKSRFAMLD<sup>41</sup>) peptide significantly reduces circulating levels of triglycerides, LDL-C, and small dense (sd)-LDL-C in *ob/ob* mice and decreases obese-induced fatty liver. Moreover, E3 vaccination does not induce cytotoxicity in *ob/ob* mice. Interestingly, the effect of E3 vaccination on dyslipidemia attenuates development of atherosclerosis in B6.KOR/*StmSlc-Apoe<sup>shl</sup>* mice fed a high-cholesterol diet, which represent a model of severe familial hypercholesterolemia (FH) caused by ApoE loss of function. Taken together, ANGPTL3 vaccination could be an effective therapeutic strategy against dyslipidemia and associated diseases.

## INTRODUCTION

Cardiovascular disease (CVD), such as ischemic heart disease and stroke, is a major cause of death worldwide (Global Health Estimates 2016. Geneva, World Health Organization; 2018). Dyslipidemia, a condition marked by hyper low-density lipoprotein (LDL) cholesterol, hypo high-density lipoprotein (HDL) cholesterol, or hyper triglyceridemia, is a critical risk factor for atherosclerosis, thereby increasing CVD development and progression.<sup>1,2</sup> For primary and secondary CVD prevention, a common therapeutic guideline is “the lower the better” in terms of lowering LDL cholesterol (LDL-C).<sup>1,2</sup> Currently, aggressive combination therapy is used to adhere to this guideline, including statins (which inhibit hydroxymethylglutaryl HMG [CoA] reductase in liver), ezetimibe (which inhibits Niemann-pick c1-like 1 (NPC1L1) protein on cells of the gastrointestinal tract), or anti-

body targeting the proprotein convertase subtilisin/kexin type 9 (PCSK9) (which regulates LDL receptor recycling).<sup>3–6</sup> Recent guidelines indicate that more intensive therapy to lower LDL-C is desirable for secondary prevention of a CVD event.<sup>1,2</sup> On the other hand, lowering plasma triglyceride (TG) levels is also important to decrease risk of CVD. The protective effect of lowering of plasma TG on CVD risk is reportedly coupled to lowering of remnant-like particle cholesterol (RLP-C)<sup>7</sup> and/or small dense low-density lipoprotein cholesterol (sd-LDL-C)<sup>8</sup> in circulation, which are both characterized as atherogenic lipoproteins.

More recently, Angiotensin-like protein (ANGPTL) 3 has received attention as a new target in strategies to lower both LDL-C and TG. ANGPTL3, a secreted protein abundantly expressed in liver, was identified from a mutant mouse exhibiting hypotriglyceridemia (KK/San mouse)<sup>9</sup> and inhibits lipoprotein



lipase (LPL), resulting in increased plasma TG.<sup>10,11</sup> Interestingly, recent papers report that humans with heterozygous or homozygous loss-of-function *ANGPTL3* variants show decreased LDL-C and TG levels in circulation without adverse symptoms.<sup>12–14</sup> Thus, CVD incidence in populations with loss-of-function *ANGPTL3* variants is significantly lower than in controls lacking these variants.<sup>13</sup> Thus, *ANGPTL3* inhibition could serve as a promising therapeutic strategy to lower risk of CVD development by antagonizing dyslipidemia and subsequent atherosclerosis. Likewise, studies of *PCSK9* loss-of-function variants provide a precedent by showing that genetic studies can faithfully predict lipid changes and CVD outcomes resulting from pharmacologic targeting of a molecule.<sup>15</sup>

Currently, anti-*ANGPTL3* antibodies, antisense oligonucleotides (ASOs), and small interfering RNAs (siRNAs) targeting *ANGPTL3* have been developed as targeted *ANGPTL3* inhibitors and are undergoing phase I–III clinical testing (ClinicalTrials.gov numbers: NCT03409744, NCT03452228, NCT03371355, NCT03747224). Among *ANGPTL3* inhibitors, anti-*ANGPTL3* antibodies reportedly have favorable effects on lipid profiles, even against treatment-resistant human homozygous familial hyperlipidemia (FH).<sup>16,17</sup> However, in general, given the economic burden of prolonged treatment with targeted drugs, antibodies, and/or ASO, use of these drugs could be difficult to implement worldwide.<sup>18</sup> Therefore, more cost-effective treatments against dyslipidemia and associated diseases are required.

To address this need, we developed a peptide vaccine effective in targeting *ANGPTL3*. To do so, we designed 3 different *ANGPTL3* epitopes for immunization and subsequently evaluated antibody production, anti-dyslipidemia phenotypes, and safety of vaccines using B6.Cg-*Lep<sup>ob</sup>*/J (*ob/ob*) mice as an obesity-associated dyslipidemia mouse model. We also evaluated whether vaccination by the optimal peptide could show anti-dyslipidemia and anti-atherosclerotic effects in B6.KOR/StmSlc-*ApoE<sup>shl</sup>* mice fed a high-cholesterol diet as a severe FH mouse model caused by *ApoE* loss of function. Finally, we examined changes in antibody titers against *ANGPTL3* after immunization to estimate vaccine durability using C57BL/6J wild-type mice.

## RESULTS

### Selection and screening of antigen sequences for an *ANGPTL3* vaccine

To optimize production of neutralizing antibodies, we selected three epitopes as candidate antigens based on the three-dimensional *ANGPTL3* structure (UniProtKB id: Q9R182, Q9Y5C1) and epitope information relevant to hydrophilicity. We designated them epitope (E) 1, amino acids (aa) 17–25; E2, aa 416–425; and E3, aa 32–41 (Figure 1A; Table S1).<sup>13,19,20</sup> Prior to injection, we conjugated each to keyhole limpet hemocyanin (KLH) to establish E1-KLH, E2-KLH, or E3-KLH. Respective peptide conjugates were mixed 1:1 with Freund's adjuvant. Then, on weeks 0, 2, and 4, we intradermally injected solutions into *ob/ob* mice ( $n = 7–12$ ), as dyslipidemia is most often seen in overweight or obese individuals. Control mice were injected with an equal quantity of KLH in Freund's adjuvant (Figure 1B).

Six weeks after the first immunization, we examined the effects of epitope candidates on production of specific antibody

in immunized mice. First, we found that antibody titers against *ANGPTL3* were significantly higher in mice immunized with E2 and E3 antigens relative to KLH controls, while the E1 group did not show a robust response (Figure 1C). Next, to evaluate specificity of antibodies in mouse sera, we performed western blot analysis against recombinant *ANGPTL3* (r*ANGPTL3*) and various BSA-conjugated peptide candidates. Sera from mice immunized with E1, E2, or E3 recognized both r*ANGPTL3* and respective E1-BSA (Figure 1D), E2-BSA (Figure 1E), or E3-BSA (Figure 1F) conjugates. By contrast, sera of KLH-immunized control mice did not recognize any peptide-BSA conjugate (Figure 1G), although all three were recognized by commercially available anti-BSA antibody (Ab) (Figure 1H). Moreover, none of the three candidate peptides had significant effects on *Angptl3* transcript levels in liver or *ANGPTL3* protein in circulation in *ob/ob* mice (Figures 1I and 1J).

### Effect of *ANGPTL3* vaccination on lipid metabolism in *ob/ob* mice exhibiting obese-induced dyslipidemia

We then asked whether *ANGPTL3* vaccination would have a favorable effect on blood lipid profiles in *ob/ob* mice. Six weeks after the first immunization with each one of the 3 epitopes, we evaluated serum TG, LDL-C, sd-LDL-C, HDL cholesterol (HDL-C), and total cholesterol (TC) levels. In the E3 group, while we observed no significant change of serum TG levels in fasting conditions, serum TG levels in non-fasting conditions significantly decreased relative to KLH controls (Figures 2A and 2B). Also in the E3 group, LDL-C and sd-LDL-C levels decreased in fasting conditions relative to KLH controls (Figures 2C and 2D), whereas serum HDL-C and TC levels tended to be lower but differences were not statistically significant (Figures 2E and 2F). By contrast, relative to KLH controls, we observed no significant impact in lipid profiles in the E1 or E2 groups (Figures 2A–2F).

Because obese-induced fatty liver is associated with TG metabolism, we evaluated vaccine effects on TG accumulation in liver of *ob/ob* mice vaccinated with E1, E2, or E3 or control KLH. Six weeks after the first immunization with the E3 vaccine, we observed no effect on body weight (BW) (Figure 3A), whereas ratios of liver weight (LW) to BW significantly decreased relative to the control KLH group (Figure 3B). Furthermore, TG accumulation in liver tissue significantly decreased in the E3 group relative to controls, while we observed no significant reduction in groups treated with E1 or E2 peptides (Figure 3C). Based on data relevant to circulating lipids or TG accumulation in liver, we conclude that the E3 peptide is the most potent anti-*ANGPTL3* vaccine. Therefore, we focused on E3 in investigating vaccine effects on fatty liver-associated pathology caused by obesity. Six weeks after the first immunization of *ob/ob* mice with E3, histological analysis revealed that steatosis, lobular inflammation, and hepatocyte ballooning, as estimated by the nonalcoholic fatty liver disease activity score (NAS),<sup>21</sup> were alleviated in E3-immunized relative to control mice (Figures 3D and 3E). Furthermore, transcript levels of *Acc1* and *Fasn*, both enzymes functioning in fatty acid (FA) synthesis in liver, and circulating free fatty acid (FFA) levels, which are sources of liver lipid droplets, significantly decreased in the E3 relative to control group (Figures 3F–3H). Moreover, circulating levels of alanine aminotransferase (ALT), a marker of liver damage, as well as

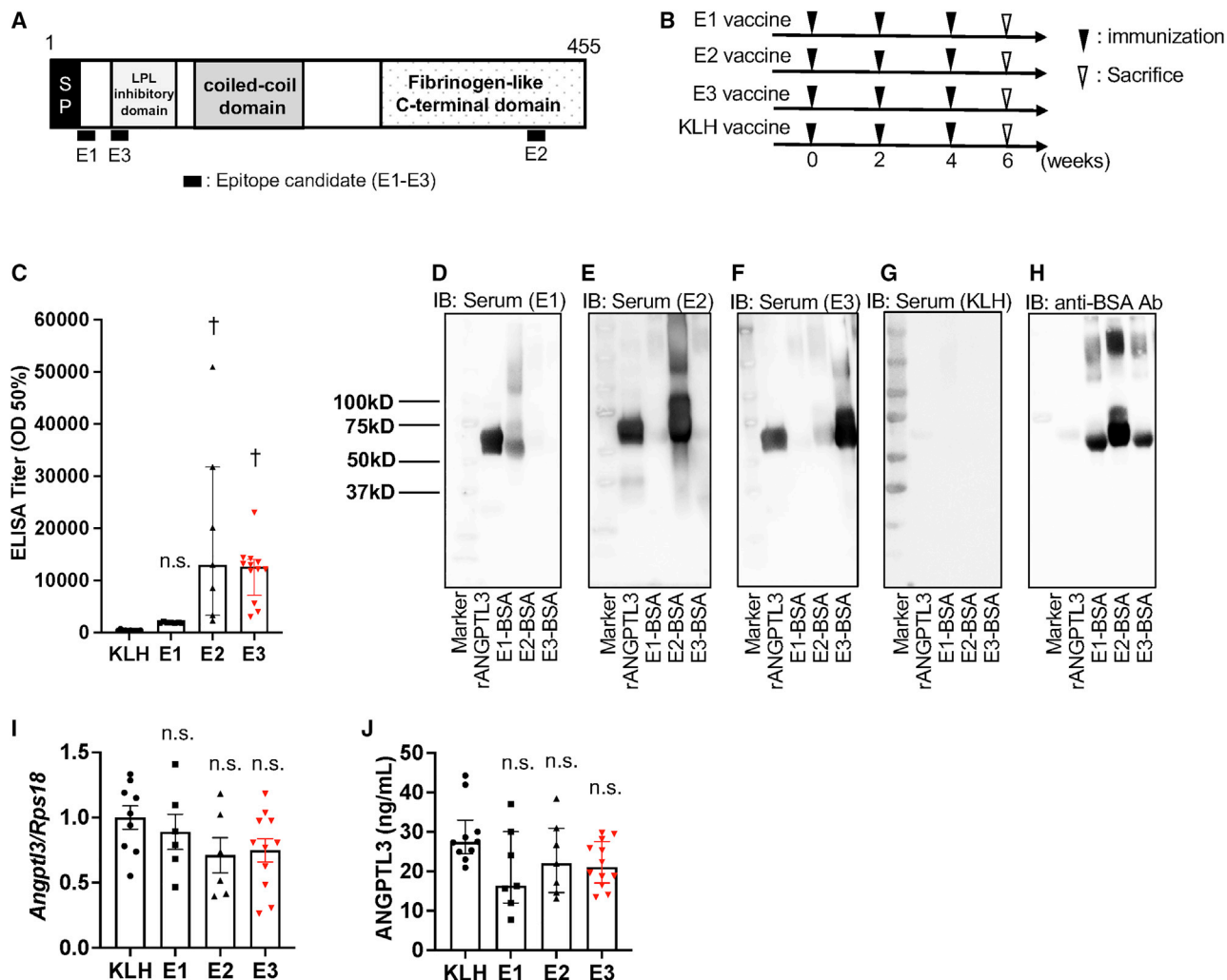


**Figure 1. Development of an ANGPTL3 vaccine**

(A) Schematic diagram of ANGPTL3 protein. Epitope candidates (E1–E3) are denoted by black bars, and functional domains are indicated. (B) Schematic showing vaccine injection protocol (black arrowheads) and animal sacrifice (open arrowheads). (C–J) Analyses of *ob/ob* mice 6 weeks after the first immunization. (C) Antibody titer following injection of indicated peptides as assessed by ELISA ( $n = 7–12$  per group). Values are reported as the serum dilution giving half-maximal binding (optical density: OD50%). (D–H) Western blots probed with sera from indicated mice (D–G) or with anti-BSA antibody (H). All 5 blots are identical and contain a molecular weight marker (lane 1), recombinant ANGPTL3 (lane 2), E1 peptide conjugated to BSA (E1-BSA) (lane 3), E2-BSA (lane 4), and E3-BSA (lane 5). IB, immunoblot; rANGPTL3, recombinant ANGPTL3. (I and J) *Angptl3* transcript levels in liver of *ob/ob* mice ( $n = 6–11$  per group) (I) and circulating ANGPTL3 concentrations in *ob/ob* mice ( $n = 7–12$  per group) (J). Transcript levels in the KLH group were set to 1. (C and J) Results are expressed as median  $\pm$  IQR. (I) Results are expressed as mean  $\pm$  SEM n.s., not significant;  $\dagger p < 0.01$  versus KLH (control) group.

levels in liver tissues of mRNAs encoding the inflammatory markers IL-6 and tumor necrosis factor (TNF)- $\alpha$ , significantly decreased in the E3 relative to control group (Figures 3I–3K). These findings suggest that ANGPTL3 vaccination could have ameliorating effects on lipid metabolism in obese pathologies.

#### Evaluation of cytotoxic autoimmune responses by ANGPTL3 vaccination in *ob/ob* mice

To determine whether E3 peptide vaccine elicits cytotoxic autoimmune responses via T cell activation, we estimated *in vitro* proliferation of T cells from mice immunized with E3 peptide vac-

cine. To do so, 6 weeks after the first immunization, we collected whole spleen cells from *ob/ob* mice immunized with the E3 peptide and cultured them *in vitro* in the presence of vehicle, KLH, E3, or positive control phytohemagglutinin (PHA). Whole spleen cells, including T cells, significantly proliferated following KLH treatment, while cells treated with E3 peptide did not show comparable proliferation (Figure 4A). As expected, cells cultured with PHA, a T cell-specific activator, showed greater proliferation than did vehicle-treated (negative control) cells (Figure 4A). Furthermore, KLH-treated cells in these cultures secreted higher levels of cytokines such as IFN- $\gamma$ , IL-2, IL-4, and IL-10 than did

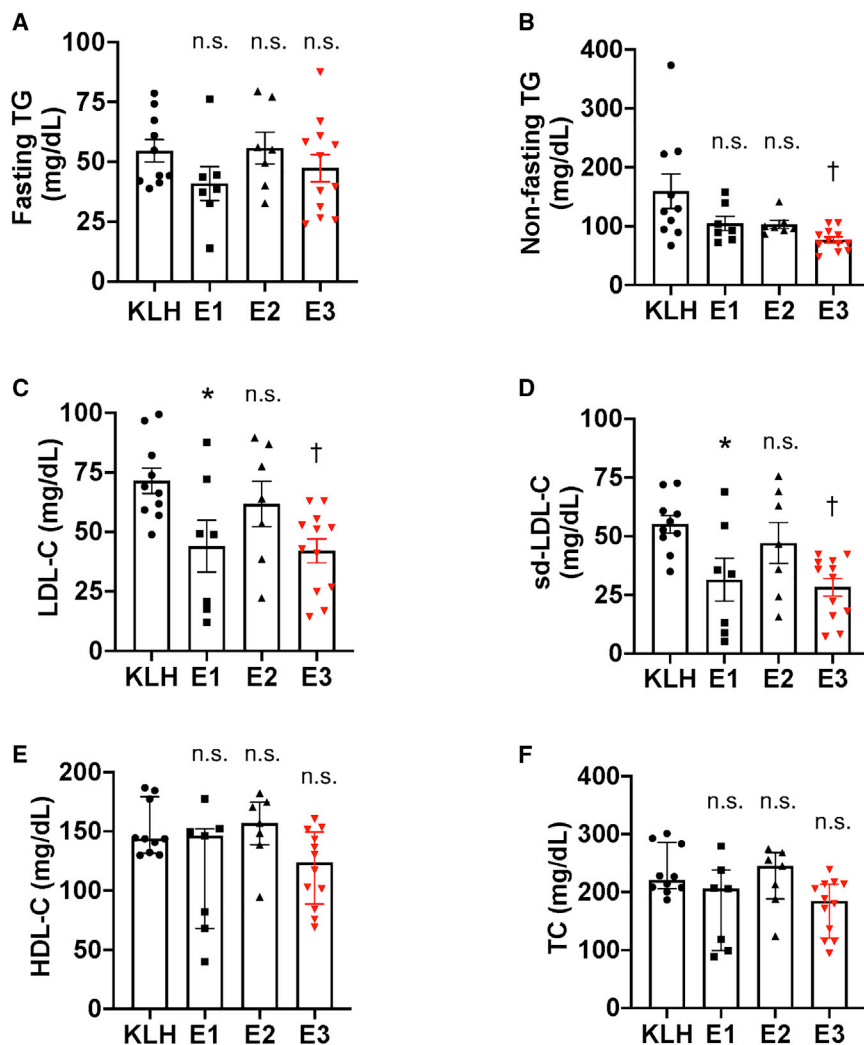


**Figure 2. Improved lipid profiles in *ob/ob* mice following ANGPTL3 vaccination**

(A–F) Levels of (A) fasting triglycerides (TG), (B) non-fasting TG, (C) fasting LDL-C, (D) fasting sd-LDL-C, (E) fasting HDL-C, and (F) fasting total cholesterol (TC) in circulation of mice 6 weeks after the first immunization (n = 7–12 per group). (A–D) Results are expressed as mean ± SEM (E and F) Results are expressed as median ± IQR. \*p < 0.05 and †p < 0.01 versus KLH (control) group.

nated with E3 peptide showed decreased serum TG levels relative to controls in non-fasting conditions, while in fasting conditions serum TG levels were comparable in vaccinated and control groups (Figures 5C and 5D). Serum VLDL-C, LDL-C, HDL-C, and TC levels decreased in fasting conditions in the E3 relative to the KLH (control) group (Figures 5E–5I), although differences in sd-LDL-C levels between the two groups were not statistically significant (Figure 5G). Overall, we conclude that lipid profiles improved in early phases after ANGPTL3 (E3) vaccination, even in a severe FH mouse model. Thus, we asked whether anti-hypercholesterolemia effects of E3 peptide vaccination would suppress atherosclerosis development in *ApoE<sup>shl</sup>* mice fed a high-cholesterol diet. By 22 weeks after the first immunization, the median size of atherosclerotic lesions seen in *ApoE<sup>shl</sup>* mice receiving the E3 vaccination was significantly smaller than lesions seen in controls (Figures 5J and 5K). These findings suggest that the ANGPTL3

cells treated with E3 peptide (Figures 4B–4E). Six weeks after the first immunization, Masson trichrome staining of liver tissues from vaccinated mice revealed that neither the E3-KLH group nor the control group that received an equal quantity of KLH in Freund’s adjuvant showed fibrotic changes, as a potential indicator of cytotoxic tissue injury (Figures 3D, 3E, 4F, 4G, and 4H). Consistently, liver tissues from the E3-KLH and KLH (control) groups showed comparable levels of transcripts of the fibrosis markers *Col1a1* and *Col3a1* (Figure 4I and 4J).

**Effect of ANGPTL3 vaccination on dyslipidemia and atherosclerosis in a severe FH mouse model**

We next asked whether ANGPTL3 vaccination with E3 peptide would have anti-dyslipidemia and/or anti-atherosclerotic effects in *ApoE<sup>shl</sup>* mice fed on high-cholesterol diet, which represent a severe FH mouse model. Six weeks after the first ANGPTL3 (E3) vaccination, we observed significantly increased antibody titers against ANGPTL3 (Figure 5A) and decreased circulating ANGPTL3 protein levels (Figure 5B). At that same time point (6 weeks), we assessed lipid profiles and found that mice vacci-

ination (E3) attenuates atherosclerosis development by improving dyslipidemia, even in a severe FH mouse model.

**Estimation of ANGPTL3 (E3) vaccination durability in mice**

Although lipid profiles improved in *ApoE<sup>shl</sup>* mice immunized with E3 antigens as compared to KLH at week 6 after vaccination (Figure 5), these differences were not significant by week 22 week after vaccination (Figure S1). Because atherosclerosis development was significantly suppressed in *ApoE<sup>shl</sup>* mice vaccinated with E3 peptide (Figures 5J and 5K), we examined durability of E3 vaccine treatment. To do so, we estimated potential fluctuation of anti-ANGPTL3 antibody titers in C57BL/6J wild-type mice following immunization with the E3 vaccine. Antibody titers against ANGPTL3 were significantly higher in mice immunized with E3 antigens relative to KLH controls at week 6 after the first immunization, and those differences remained statistically significant until week 30 (Figure 6A). Likewise, therapeutic efficacy in lowering serum TG levels seen in the E3 group continued until 30 weeks after vaccination in wild-type mice

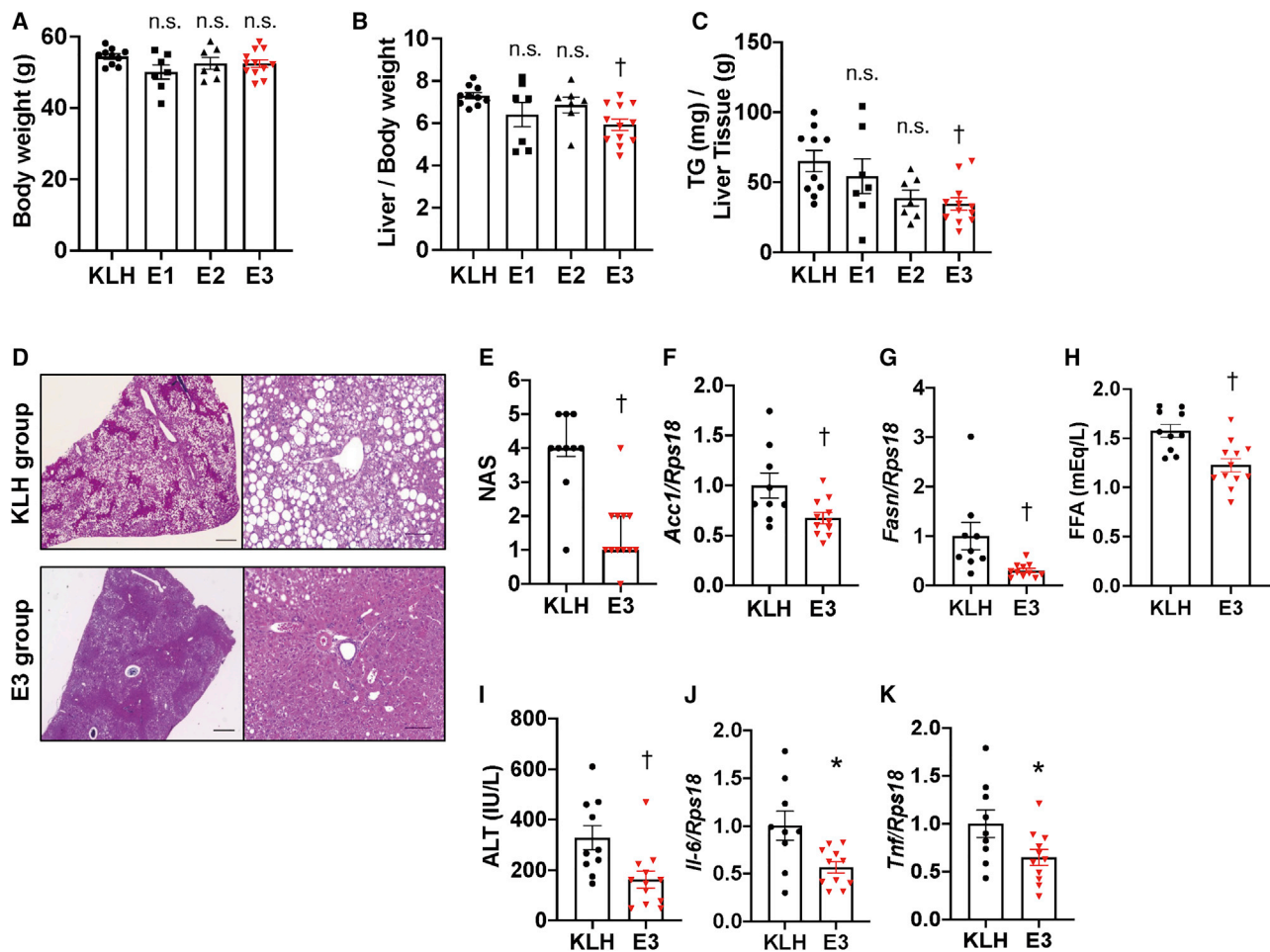


**Figure 3. Decreased TG accumulation in liver of *ob/ob* mice following ANGPTL3 vaccination**

(A–K) Analyses of *ob/ob* mice 6 weeks after the first immunization. (A) Body weight (n = 7–12 per group). (B) Liver weight/body weight (%) (n = 7–12 per group). (C) TG content in liver (n = 7–12 per group). (D) Representative images of hematoxylin and eosin (H&E)-stained liver sections. Scale bars, 500 (left) and 100  $\mu$ m (right). (E) Nonalcoholic fatty liver disease activity score (NAS), as estimated based on H&E-stained sections (n = 7–12 per group). (F and G) Quantitative real-time PCR in liver tissue of mRNAs encoding factors functioning in hepatic lipogenesis (KLH: n = 9, E3: n = 11). KLH group values were set to 1. (H) Circulating free fatty acid (FFA) levels (KLH: n = 10, E3: n = 12). (I) Serum alanine aminotransferase (ALT) levels (KLH: n = 10, E3: n = 12). (J and K) Transcript levels of (J) IL-6 and (K) TNF- $\alpha$  in liver tissues (KLH: n = 9, E3: n = 11). KLH group values were set to 1.

(A–C, F, and H–K) Results are expressed as mean  $\pm$  SEM (E and G). Results are expressed as median  $\pm$  IQR. n.s., not significant; \*p < 0.05 and †p < 0.01 versus KLH (control) group.

(Figure 6B). Thus, we estimate vaccine durability to be  $\sim$ 30 weeks. Notably, we observed no differences in body weight between mice immunized with E3 antigens and KLH controls throughout the observation period, suggesting a lack of cytotoxic effects by the vaccine (Figure 6C).

#### Effect of ANGPTL3 vaccination on circulating ANGPTL8 levels

Since ANGPTL3 reportedly regulates plasma TG levels by forming a complex with ANGPTL8,<sup>22</sup> we investigated circulating ANGPTL8 levels in *ob/ob* mice after ANGPTL3 vaccination. Six weeks after E3 peptide immunization, circulating ANGPTL8 levels were comparable to those seen in controls (Figure 7A). On the other hand, 6 weeks after E3 peptide immunization of *ApoE<sup>shl</sup>* mice, circulating ANGPTL8 levels significantly increased

relative to controls (Figure 7B). Taken together, ANGPTL3 vaccination may increase circulating ANGPTL8 levels in mice depending on context.

#### DISCUSSION

Here, we generated a peptide vaccine targeting ANGPTL3 aa 32–41 (E3), which improved dyslipidemia in mice. First, the E3 vaccination decreased circulating levels of TG, LDL-C, and sd-LDL-C in *ob/ob* mice, an obese-induced dyslipidemia model.<sup>13,19,20</sup> The mouse E3 peptide amino acid sequence is identical to the corresponding human sequence (UniProtKB id: Q9R182, Q9Y5C1), suggesting that this peptide could potentially be investigated in clinical studies. Second, treatment with E3 vaccine reduced TG accumulation in mouse hepatocytes but

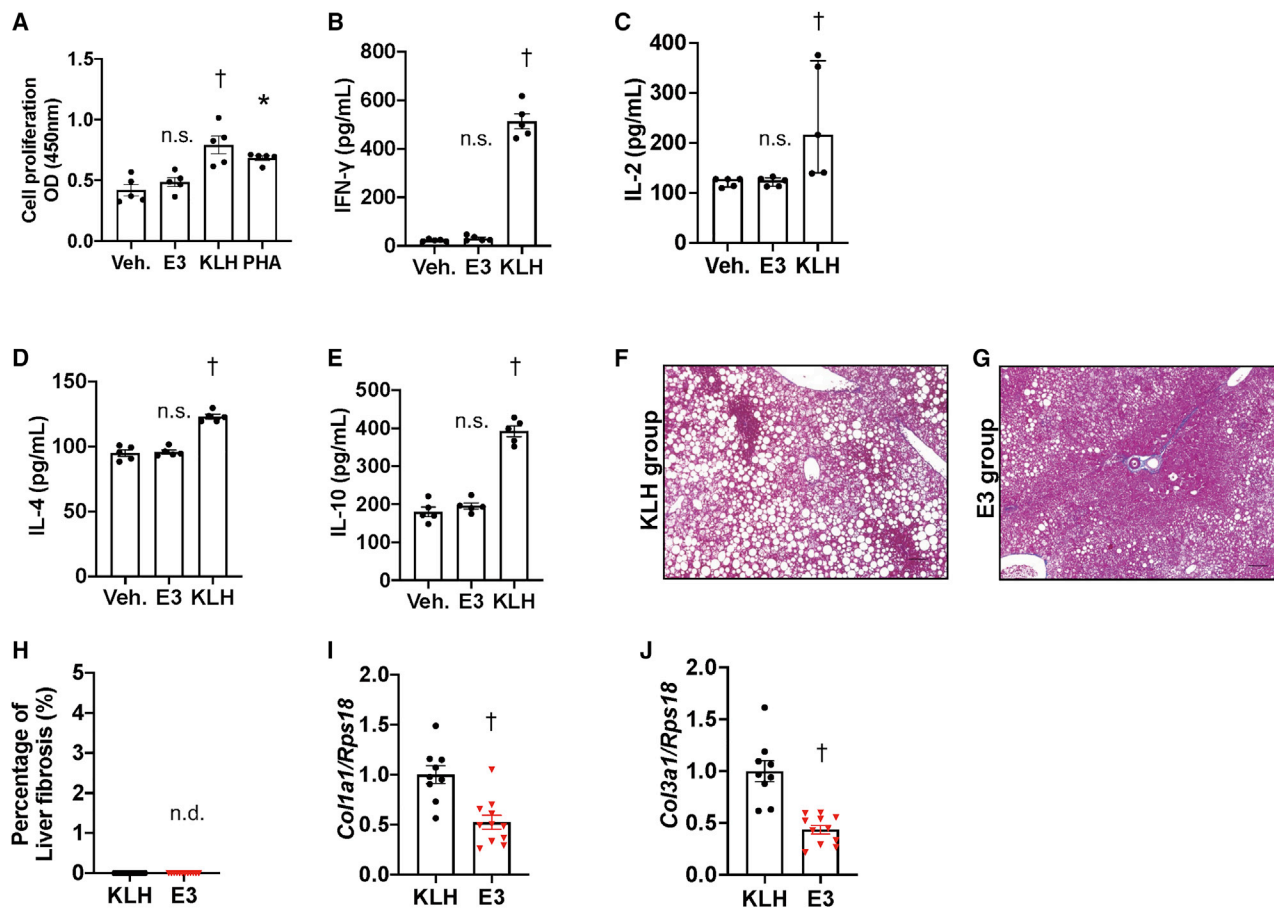


**Figure 4. Evaluation of cytotoxic autoimmune responses following ANGPTL3 vaccination in *ob/ob* mice**

(A–J) Analyses of T cells and liver from *ob/ob* mice 6 weeks after the first immunization. (A) T cell proliferation assay of immunized mouse spleen cells performed 48 h after supplementation of culture media with vehicle, E3, KLH, or PHA ( $n = 5$  per group). (B–E) Concentrations of (B) IFN- $\gamma$ , (C) IL-2, (D) IL-4, and (E) IL-10 in culture supernatants ( $n = 5$  per group).

(F and G) Representative images of Azan-Mallory-stained liver sections from (F) KLH and (G) E3 groups. Scale bars, 200  $\mu\text{m}$ .

(H) Percentages of aniline blue-positive interstitial areas indicate degree of liver fibrosis.

(I and J) Transcript levels of (I) *Col1a1* and (J) *Col3a1* in liver. Transcript levels were normalized to *Rps18* levels. KLH group values were set to 1.

(A, B, D, E, I, and J) Results are expressed as mean  $\pm$  SEM (C) Results are expressed as median  $\pm$  IQR. Veh, vehicle; n.s., not significant; \* $p < 0.05$ , † $p < 0.01$  versus control.

induced no major cytotoxic autoimmune responses. Third, E3 vaccination attenuated atherosclerosis development based on improving dyslipidemia even in *ApoE<sup>sh1</sup>* mice fed a high-cholesterol diet, a mouse model of severe familial hypercholesterolemia. Finally, antibody production induced by E3 vaccination continued for approximately 30 weeks after initial immunization in mice. We conclude overall that the ANGPTL3 (E3) peptide vaccine could be an effective therapeutic strategy against dyslipidemia and associated diseases.

Current guidelines recommend lowering LDL-C in conditions of hyper LDL cholesterolemia.<sup>1,2</sup> Pharmaceutical ANGPTL3 suppression lowers circulating LDL-C levels, even in FH patients who have undergone aggressive combination therapy with a statin and a PCSK9 inhibitor,<sup>17</sup> strongly suggesting that these reductions do not depend on increasing LDL receptor expression levels. Moreover, lipid profiles improve following ANGPTL3 inhibition in FH patients previously treated with ezetimibe,<sup>17</sup> sug-

gesting that anti-ANGPTL3 treatment may target mechanisms not targeted by other available therapies. Consistently, LDL-C decreases seen following ANGPTL3 inhibition are reportedly independent of activities related to LDL receptor-related protein 1, apolipoprotein E, syndecan 1, or the LDL receptor.<sup>23</sup> Currently available drugs whose mechanism of action largely depends on upregulated LDL-receptor function do not typically achieve guideline-recommended target LDL-C levels, particularly in FH patients.<sup>24</sup> Lomitapide and mipomersen, however, do act independently of LDL-receptor function, but their wide application is limited by adverse effects.<sup>24,25</sup> Accordingly, ANGPTL3 is a candidate target for novel strategies targeting different mechanisms underlying hyper LDL cholesterolemia.

Nonetheless, in some dyslipidemia patients whose circulating LDL-C levels are lowered by medication, higher circulating TG levels remain a risk factor for CVD.<sup>26</sup> Some types of genetic or drug-mediated ANGPTL3 suppression lower circulating levels

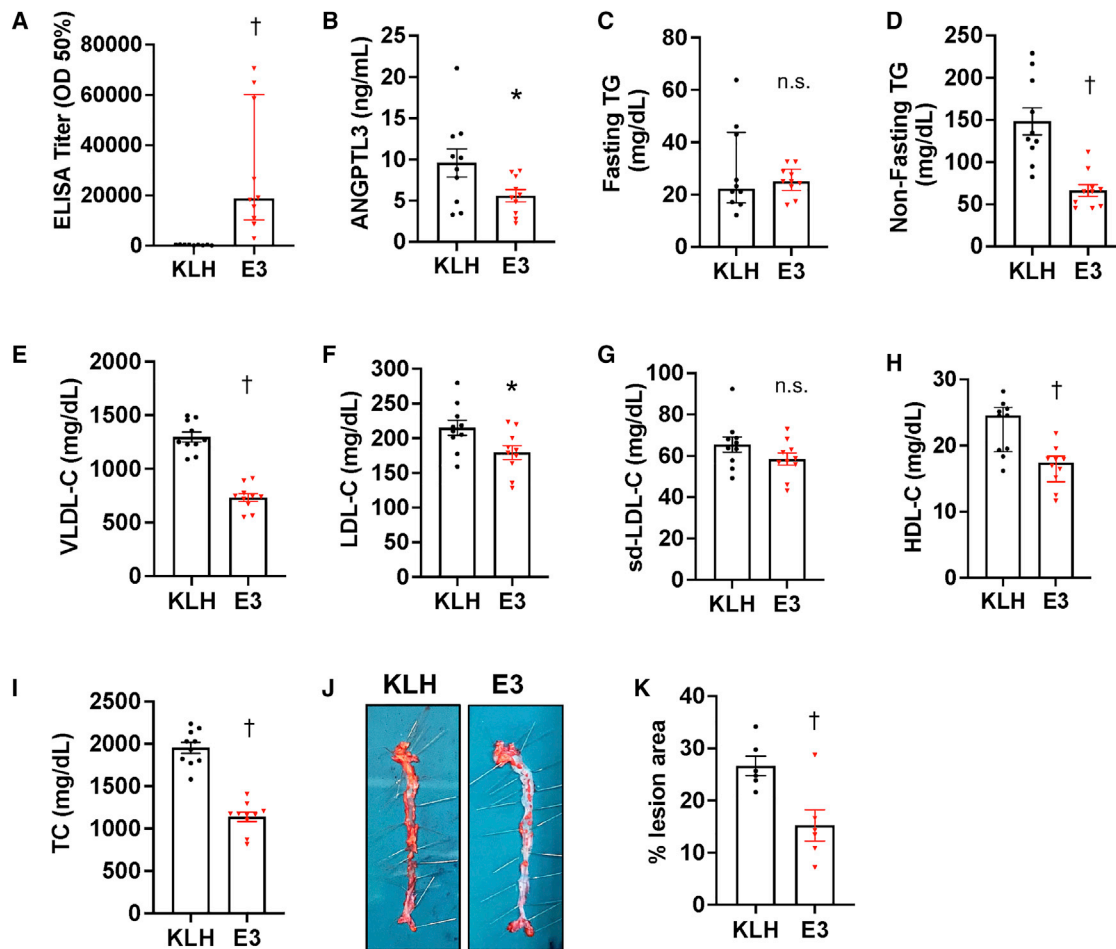


**Figure 5. Improved lipid profiles in severe familial hypercholesterolemia model mice following ANGPTL3 vaccination**

(A–I) Blood samples from *ApoE<sup>shl</sup>* mice fed a high-cholesterol diet were analyzed 6 weeks after the first immunization (n = 10 per group). (A) Titers of circulating antibodies. Values are reported as the serum dilution giving half-maximal binding (optical density: OD50%). (B) Circulating ANGPTL3 concentrations. (C–I) Levels of (C) fasting TG, (D) non-fasting TG, (E) fasting VLDL-C, (F) fasting LDL-C, (G) fasting sd-LDL-C, (H) fasting HDL-C, and (I) fasting TC in circulation.

(J and K) Evaluation of atherosclerotic plaques in aorta from *ApoE<sup>shl</sup>* mice fed a high-cholesterol diet. Analysis was performed 22 weeks after the first immunization (n = 6 per group). (J) Representative photographs of Oil red O-stained aortas of indicated mice. (K) Quantitative comparison of disease severity based on atherosclerotic lesion area. (A, C, and H) Results are expressed as median ± IQR.

(B, D–G, I, and K) Results are expressed as mean ± SEM. \*p < 0.05 and †p < 0.01 versus KLH (control) group.

of LDL-C and TG in human subjects.<sup>13,16,17,27</sup> Here, we demonstrated that ANGPTL3 vaccination significantly decreased circulating levels of both LDL-C and non-fasting TG in both *ob/ob* mice and *ApoE<sup>shl</sup>* mice. Also, since lower TG levels in non-fasting conditions are more associated with reduction of future CVD development relative to outcomes in fasting conditions,<sup>28</sup> targeting ANGPTL3 could reduce CVD risk by improving lipid metabolism, and E3 vaccination in this effort is a promising strategy.

We also found that durability of E3 vaccine treatment, defined as the period in which neutralizing antibodies are present and circulating TG concentrations remain lowered, was ~30 weeks in wild-type mice. We found that vaccine efficacy against dyslipidemia also declined by 30 weeks after immunization. We note that, in *ApoE<sup>shl</sup>* mice, therapeutic efficacy against dyslipidemia was minimal by 22 weeks after vaccination (Figure S1), sug-

gesting that decreasing antibody titers against ANGPTL3 lower serum TG levels in wild-type mice but are not sufficient to counteract dyslipidemia in a severe hyperlipidemia model. Aggressive combination therapy with other anti-dyslipidemia drugs may be necessary to achieve anti-atherosclerotic effects in the case of severe dyslipidemia subjects such as FH. Re-immunization every 5 or 6 months could maintain therapeutic efficacy of this form of ANGPTL3 (E3) vaccine therapy, and further investigation is necessary to determine whether an ANGPTL3 vaccine booster would prolong vaccine durability. Toward clinical application, we will modify the vaccine formulation (i.e., KLH carrier or adjuvants) and optimize the dosage and administration for clinical trials. Antibody therapies against dyslipidemia, such as the ANGPTL3 monoclonal antibody (mAb) Evinacumab or PCSK9 mAbs, require monthly injections,<sup>17,29</sup> while ANGPTL3 siRNA therapy



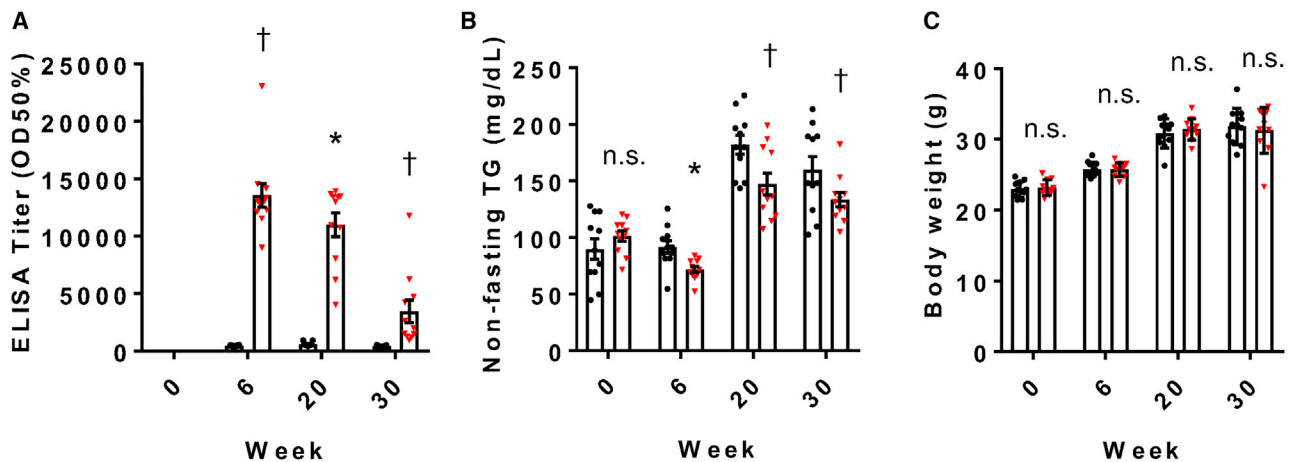


**Figure 6. ANGPTL3 vaccine durability as assessed in C57BL/6J mice**

(A) Circulating antibody titers of mice at 6, 20, and 30 weeks after the first E3 immunization. Values are reported as the serum dilution giving half-maximal binding (optical density: OD50%).  $p < 0.01$  for interaction between week and E3 treatment ( $n = 11$  per group). (B) Non-fasting TG levels in circulation of mice before immunization and at 6, 20, and 30 weeks after the first E3 immunization.  $p < 0.01$  for interaction between week and E3 treatment ( $n = 11$  per group). (C) Body weight of mice before immunization and at 6, 20, and 30 weeks after the first E3 immunization ( $n = 11$  per group).  $p = 0.88$  for interaction between week and E3 treatment. Results are expressed as mean  $\pm$  SEM. n.s., not significant. \* $p < 0.05$  versus KLH (control) group. † $p < 0.01$  versus KLH (control) group.

is effective for up to 6 months after injection.<sup>30</sup> Overall, ANGPTL3 vaccination currently appears comparable in terms of durability and frequency of administration to anti-dyslipidemia therapy antibodies or siRNA against ANGPTL3, which are often expensive compared to vaccine therapies.<sup>18,31,31</sup> Thus, the use of anti-ANGPTL3 vaccine might be a more cost-effective treatment for dyslipidemia, which can be proposed as the therapeutic option for patients.

Interestingly, E3 immunization reduced TG accumulation in hepatocytes in *ob/ob* obese mice. Both circulating FFA and newly synthesized FFA are major sources of TG accumulation in hepatocytes.<sup>32</sup> We show that both circulating FFA levels and expression of genes encoding liver enzymes involved in fatty acid synthesis, such as *Acc1* or *Fasn*, decrease in *ob/ob* obese mice following ANGPTL3 vaccination. In addition, hepatocyte damage (evaluated by ALT expression) and liver inflammation (estimated by IL-6 and TNF- $\alpha$  expression) were also attenuated in *ob/ob* obese mice following ANGPTL3 vaccination (Figure 3). Since initiation of nonalcoholic fatty liver disease (NAFLD) is caused by lipid accumulation in the liver, and often occurs in overweight or obese people,<sup>21,32</sup> ANGPTL3 might be a candidate target for drug development relevant to NAFLD. Given that *ob/ob* mice develop simple fatty liver but do not progress to fibrosis or liver cirrhosis/hepatocellular carcinoma, our future analysis will investigate whether ANGPTL3 vaccination ameliorates NAFLD in a bona fide NAFLD mouse model.

ANGPTL3 transcription in liver is minimally altered by fasting or feeding.<sup>33,34</sup> On the other hand, ANGPTL3 reportedly regulates plasma TG levels through forming a complex with ANGPTL8,<sup>22</sup> and ANGPTL8 levels increase in liver in feeding conditions.<sup>33,34</sup> Circulating TG levels decrease in both ANGPTL3 vaccine-treated *ob/ob* mice and *Apoe<sup>shl</sup>* mice in non-fasting conditions,

while we observed no significant decreases in fasting conditions. In E3-immunized *Apoe<sup>shl</sup>* mice circulating ANGPTL8 levels increased compared with controls. Thus, it may be of interest to determine whether ANGPTL3 vaccination impacts ANGPTL3/ANGPTL8 complex formation and if so whether this activity contributes to anti-dyslipidemia effects.

In summary, we established anti-dyslipidemia vaccine therapy targeting ANGPTL3, which could be an effective therapeutic strategy against dyslipidemia and associated diseases. Because the durability of KLH-conjugated E3 peptide vaccination was approximately 30 weeks in mice, further work is required to prolong vaccination efficacy as a means to improve the cost-effectiveness and increase adherence to treatment.

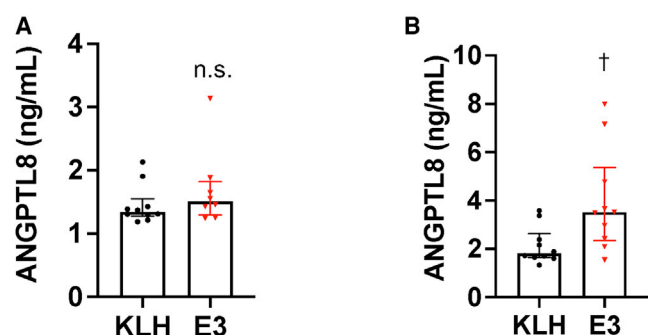


**Figure 7. Effects of ANGPTL3 vaccine on circulating ANGPTL8 levels**

(A and B) Circulating ANGPTL8 protein levels in (A) *ob/ob* (KLH [control]:  $n = 10$ , E3:  $n = 8$ ) and (B) *Apoe<sup>shl</sup>* ( $n = 10$  per group) mice at 6 weeks after the first immunization. Results are expressed as median  $\pm$  IQR., n.s., not significant., \* $p < 0.05$  versus KLH group.

### Limitations of study

This study reports proof of concept of an ANGPTL3 vaccine to treat dyslipidemia and associated diseases in mice. Prior to clinical application, further pre-clinical investigations using bona fide disease models of large animals are needed. Furthermore, because the durability of KLH-conjugated E3 peptide vaccination was approximately 30 weeks in mice, further work is required to prolong vaccination efficacy as a means to improve cost-effectiveness and increase adherence to treatment.

### STAR★METHODS

Detailed methods are provided in the online version of this paper and include the following:

- **KEY RESOURCES TABLE**
- **RESOURCE AVAILABILITY**
  - Lead contact
  - Materials availability
  - Data and code availability
- **METHOD DETAILS**
  - Vaccine design and synthesis
  - Animal studies and immunization
  - Obese-induced dyslipidemia mouse model
  - Severe familial hypercholesterolemia (FH) mouse model
  - Evaluation of ANGPTL3 vaccine durability
  - Evaluation of anti-ANGPTL3 antibody titers in immunized mice
  - Western blot analysis
  - Real-time polymerase chain reaction analysis
  - Blood chemistry
  - Measurement of liver TG
  - Histological analysis
  - Evaluation of atherosclerosis progression
  - T cell proliferation assay
  - Measurement of serum ANGPTL3 and ANGPTL8 levels
  - Statistical analysis

### SUPPLEMENTAL INFORMATION

Supplemental information can be found online at <https://doi.org/10.1016/j.xcrm.2021.100446>.

### ACKNOWLEDGMENTS

We thank our colleagues for valuable suggestions and discussion. We also thank K. Tabu, K. Saito, S. Iwaki, Y. Itoh, N. Shirai, and M. Kamada for technical assistance. This work was supported by JSPS KAKENHI (Grant Number 21K20935 to H.F.) and by the Center for Metabolic Regulation of Healthy Aging of Kumamoto University (to H.F. and to Y. Oike).

### AUTHOR CONTRIBUTIONS

Conceptualization, H.F., J.M., H.N., and Y. Oike; methodology, H.F., J.M., H.N., H. Hayashi, and Y. Oike; investigation and data collection, H.F., J.M., Y. Okadome, E.M., T. Kadomatsu, H. Horiguchi, and M.S.; statistical analysis, H.F., J.M., T.S., and K.S.; supervision, T. Kuwabara, M.M., R.M., H.N., and Y. Oike; writing – original draft, H.F., J.M., and Y. Oike; writing – review & editing, H.F., J.M., H.N., and Y. Oike.

### DECLARATION OF INTERESTS

The authors declare no competing interests.

Received: October 9, 2020

Revised: October 4, 2021

Accepted: October 19, 2021

Published: November 16, 2021

### REFERENCES

1. Grundy, S.M., Stone, N.J., Bailey, A.L., Beam, C., Birtcher, K.K., Blumenthal, R.S., Braun, L.T., de Ferranti, S., Faiella-Tommasino, J., Forman, D.E., et al. (2019). 2018 AHA/ACC/AACVPR/AAPA/ABC/ACPM/ADA/AGS/APhA/ASPC/NLA/PCNA Guideline on the Management of Blood Cholesterol: A Report of the American College of Cardiology/American Heart Association Task Force on Clinical Practice Guidelines. *Circulation* 139, e1082–e1143.
2. Mach, F., Baigent, C., Catapano, A.L., Koskinas, K.C., Casula, M., Badimon, L., Chapman, M.J., De Backer, G.G., Delgado, V., Ference, B.A., et al.; ESC Scientific Document Group (2020). 2019 ESC/EAS Guidelines for the management of dyslipidaemias: lipid modification to reduce cardiovascular risk. *Eur. Heart J.* 41, 111–188.
3. Baigent, C., Blackwell, L., Emberson, J., Holland, L.E., Reith, C., Bhalra, N., Peto, R., Barnes, E.H., Keech, A., Simes, J., and Collins, R.; Cholesterol Treatment Trialists' (CTT) Collaboration (2010). Efficacy and safety of more intensive lowering of LDL cholesterol: a meta-analysis of data from 170,000 participants in 26 randomised trials. *Lancet* 376, 1670–1681.
4. Cannon, C.P., Blazing, M.A., Giugliano, R.P., McCagg, A., White, J.A., Theroux, P., Darius, H., Lewis, B.S., Ophuis, T.O., Jukema, J.W., et al.; IMPROVE-IT Investigators (2015). Ezetimibe added to statin therapy after acute coronary syndromes. *N. Engl. J. Med.* 372, 2387–2397.
5. Sabatine, M.S., Giugliano, R.P., Keech, A.C., Honarpour, N., Wiviott, S.D., Murphy, S.A., Kuder, J.F., Wang, H., Liu, T., Wasserman, S.M., et al.; FOURIER Steering Committee and Investigators (2017). Evolocumab and clinical outcomes in patients with cardiovascular disease. *N. Engl. J. Med.* 376, 1713–1722.
6. Sabatine, M.S. (2019). PCSK9 inhibitors: clinical evidence and implementation. *Nat. Rev. Cardiol.* 16, 155–165.
7. Sandesara, P.B., Virani, S.S., Fazio, S., and Shapero, M.D. (2019). The Forgotten Lipids: Triglycerides, Remnant Cholesterol, and Atherosclerotic Cardiovascular Disease Risk. *Endocr. Rev.* 40, 537–557.
8. Ikezaki, H., Lim, E., Cupples, L.A., Liu, C.T., Asztalos, B.F., and Schaefer, E.J. (2021). Small Dense Low-Density Lipoprotein Cholesterol Is the Most Atherogenic Lipoprotein Parameter in the Prospective Framingham Offspring Study. *J. Am. Heart Assoc.* 10, e019140.
9. Koishi, R., Ando, Y., Ono, M., Shimamura, M., Yasuno, H., Fujiwara, T., Horikoshi, H., and Furukawa, H. (2002). Angptl3 regulates lipid metabolism in mice. *Nat. Genet.* 30, 151–157.
10. Shimizugawa, T., Ono, M., Shimamura, M., Yoshida, K., Ando, Y., Koishi, R., Ueda, K., Inaba, T., Minekura, H., Kohama, T., and Furukawa, H. (2002). ANGPTL3 decreases very low density lipoprotein triglyceride clearance by inhibition of lipoprotein lipase. *J. Biol. Chem.* 277, 33742–33748.
11. Oike, Y., Akao, M., Kubota, Y., and Suda, T. (2005). Angiopietin-like proteins: potential new targets for metabolic syndrome therapy. *Trends Mol. Med.* 11, 473–479.
12. Musunuru, K., Pirruccello, J.P., Do, R., Peloso, G.M., Guiducci, C., Sougnez, C., Garimella, K.V., Fisher, S., Abreu, J., Barry, A.J., et al. (2010). Exome sequencing, ANGPTL3 mutations, and familial combined hypolipidemia. *N. Engl. J. Med.* 363, 2220–2227.
13. Dewey, F.E., Gusarova, V., Dunbar, R.L., O'Dushlaine, C., Schurmann, C., Gottesman, O., McCarthy, S., Van Hout, C.V., Bruse, S., Dansky, H.M., et al. (2017). Genetic and Pharmacologic Inactivation of ANGPTL3 and Cardiovascular Disease. *N. Engl. J. Med.* 377, 211–221.

14. Minicocci, I., Montali, A., Robciuc, M.R., Quagliarini, F., Censi, V., Labbadia, G., Gabiati, C., Pigna, G., Sepe, M.L., Pannoza, F., et al. (2012). Mutations in the ANGPTL3 gene and familial combined hypolipidemia: a clinical and biochemical characterization. *J. Clin. Endocrinol. Metab.* *97*, E1266–E1275.
15. Ooi, T.C., Krysa, J.A., Chaker, S., Abujrad, H., Mayne, J., Henry, K., Cousins, M., Raymond, A., Favreau, C., Taljaard, M., et al. (2017). The effect of PCSK9 loss-of-function variants on the postprandial lipid and APOB-lipoprotein response. *J. Clin. Endocrinol. Metab.* *102*, 3452–3460.
16. Banerjee, P., Chan, K.C., Tarabocchia, M., Benito-Vicente, A., Alves, A.C., Uribe, K.B., Bourbon, M., Skiba, P.J., Pordy, R., Gipe, D.A., et al. (2019). Functional analysis of LDLR (low-density lipoprotein receptor) variants in patient lymphocytes to assess the effect of evinacumab in homozygous familial hypercholesterolemia patients with a spectrum of LDLR activity. *Arterioscler. Thromb. Vasc. Biol.* *39*, 2248–2260.
17. Raal, F.J., Rosenson, R.S., Reeskamp, L.F., Hovingh, G.K., Kastelein, J.J.P., Rubba, P., Ali, S., Banerjee, P., Chan, K.-C., Gipe, D.A., et al.; ELIPSE HoFH Investigators (2020). Evinacumab for Homozygous Familial Hypercholesterolemia. *N. Engl. J. Med.* *383*, 711–720.
18. Kazi, D.S., Moran, A.E., Coxson, P.G., Penko, J., Ollendorf, D.A., Pearson, S.D., Tice, J.A., Guzman, D., and Bibbins-Domingo, K. (2016). Cost-Effectiveness of PCSK9 inhibitor therapy in patients with heterozygous familial hypercholesterolemia or atherosclerotic cardiovascular disease. *JAMA* *316*, 743–753.
19. Biterova, E., Esmaeili, M., Alanen, H.I., Saarinen, M., and Ruddock, L.W. (2018). Structures of Angptl3 and Angptl4, modulators of triglyceride levels and coronary artery disease. *Sci. Rep.* *8*, 6752.
20. Lee, E.C., Desai, U., Gololobov, G., Hong, S., Feng, X., Yu, X.C., Gay, J., Wilganowski, N., Gao, C., Du, L.L., et al. (2009). Identification of a new functional domain in angiotensin-like 3 (ANGPTL3) and angiotensin-like 4 (ANGPTL4) involved in binding and inhibition of lipoprotein lipase (LPL). *J. Biol. Chem.* *284*, 13735–13745.
21. Kleiner, D.E., Brunt, E.M., Van Natta, M., Behling, C., Contos, M.J., Cummings, O.W., Ferrell, L.D., Liu, Y.C., Torbenson, M.S., Unalp-Arida, A., et al.; Nonalcoholic Steatohepatitis Clinical Research Network (2005). Design and validation of a histological scoring system for nonalcoholic fatty liver disease. *Hepatology* *41*, 1313–1321.
22. Chi, X., Britt, E.C., Shows, H.W., Hjelmaas, A.J., Shetty, S.K., Cushing, E.M., Li, W., Dou, A., Zhang, R., and Davies, B.S.J. (2017). ANGPTL8 promotes the ability of ANGPTL3 to bind and inhibit lipoprotein lipase. *Mol. Metab.* *6*, 1137–1149.
23. Wang, Y., Gusarova, V., Banfi, S., Gromada, J., Cohen, J.C., and Hobbs, H.H. (2015). Inactivation of ANGPTL3 reduces hepatic VLDL-triglyceride secretion. *J. Lipid Res.* *56*, 1296–1307.
24. Blom, D.J., Cuchel, M., Ager, M., and Phillips, H. (2018). Target achievement and cardiovascular event rates with Lomitapide in homozygous Familial Hypercholesterolemia. *Orphanet J. Rare Dis.* *13*, 96.
25. Reeskamp, L.F., Kastelein, J.J.P., Moriarty, P.M., Duell, P.B., Catapano, A.L., Santos, R.D., and Ballantyne, C.M. (2019). Safety and efficacy of mipomersen in patients with heterozygous familial hypercholesterolemia. *Atherosclerosis* *280*, 109–117.
26. Griffin, B.A., Freeman, D.J., Tait, G.W., Thomson, J., Caslake, M.J., Packard, C.J., and Shepherd, J. (1994). Role of plasma triglyceride in the regulation of plasma low density lipoprotein (LDL) subfractions: relative contribution of small, dense LDL to coronary heart disease risk. *Atherosclerosis* *106*, 241–253.
27. Graham, M.J., Lee, R.G., Brandt, T.A., Tai, L.J., Fu, W., Peralta, R., Yu, R., Hurh, E., Paz, E., McEvoy, B.W., et al. (2017). Cardiovascular and metabolic effects of ANGPTL3 antisense oligonucleotides. *N. Engl. J. Med.* *377*, 222–232.
28. Bansal, S., Buring, J.E., Rifai, N., Mora, S., Sacks, F.M., and Ridker, P.M. (2007). Fasting compared with nonfasting triglycerides and risk of cardiovascular events in women. *JAMA* *298*, 309–316.
29. Rosenson, R.S., Hegele, R.A., Fazio, S., and Cannon, C.P. (2018). The Evolving Future of PCSK9 Inhibitors. *J. Am. Coll. Cardiol.* *72*, 314–329.
30. Nordestgaard, B.G., Nicholls, S.J., Langsted, A., Ray, K.K., and Tybjaerg-Hansen, A. (2018). Advances in lipid-lowering therapy through gene-silencing technologies. *Nat. Rev. Cardiol.* *15*, 261–272.
31. Rüger, J., Ioannou, S., Castanotto, D., and Stein, C.A. (2020). Oligonucleotides to the (Gene) Rescue: FDA Approvals 2017–2019. *Trends Pharmacol. Sci.* *41*, 27–41.
32. Tamura, S., and Shimomura, I. (2005). Contribution of adipose tissue and de novo lipogenesis to nonalcoholic fatty liver disease. *J. Clin. Invest.* *115*, 1139–1142.
33. Quagliarini, F., Wang, Y., Kozlitina, J., Grishin, N.V., Hyde, R., Boerwinkle, E., Valenzuela, D.M., Murphy, A.J., Cohen, J.C., and Hobbs, H.H. (2012). Atypical angiotensin-like protein that regulates ANGPTL3. *Proc. Natl. Acad. Sci. USA* *109*, 19751–19756.
34. Haller, J.F., Mintah, I.J., Shihanian, L.M., Stevis, P., Buckler, D., Alexa-Braun, C.A., Kleiner, S., Banfi, S., Cohen, J.C., Hobbs, H.H., et al. (2017). ANGPTL8 requires ANGPTL3 to inhibit lipoprotein lipase and plasma triglyceride clearance. *J. Lipid Res.* *58*, 1166–1173.
35. Pang, Z., Nakagami, H., Osako, M.K., Koriyama, H., Nakagami, F., Tomioka, H., Shimamura, M., Kurinami, H., Takami, Y., Morishita, R., and Rukugi, H. (2014). Therapeutic vaccine against DPP4 improves glucose metabolism in mice. *Proc. Natl. Acad. Sci. USA* *111*, E1256–E1263.

STAR★METHODS

KEY RESOURCES TABLE

| Reagent or resource   | Source                                  | Identifier                         |
|---|---|------------------------------------|
| <b>Antibody</b>   |   |                                    |
| anti-Bovine Serum Albumin (BSA) antibody                      | Abcam                                   | Cat# ab79827, RRID:AB_1603068      |
| Sheep anti-Mouse IgG - Horseradish Peroxidase antibody        | GE Healthcare                           | Cat# NA931, RRID:AB_772210         |
| <b>Chemicals, peptides, and recombinant proteins</b>          |   |                                    |
| Angiotensin-like 3 (ANGPTL3) peptide                          | Peptide Institute                       | N/A                                |
| BSA conjugated to ANGPTL3 peptide                             | Peptide Institute                       | N/A                                |
| keyhole limpet hemocyanin (KLH) conjugated to ANGPTL3 peptide | Peptide Institute                       | N/A                                |
| KLH   | G-BIOSCIENCES                           | Cat# 786-088 CAS No.9013-72-3      |
| Freund's Complete Adjuvant                                    | FUJIFILM Wako Pure Chemical Corporation | Cat# 014-09541                     |
| Freund's Incomplete Adjuvant                                  | FUJIFILM Wako Pure Chemical Corporation | Cat# 011-09551                     |
| Recombinant Mouse ANGPTL3 Protein                             | R&D Systems                             | Cat# 136-AN                        |
| RPMI-1640   | FUJIFILM Wako Pure Chemical Corporation | Cat# 189-02025                     |
| Fetal Bovine Serum (FBS)                                      | Sigma-Aldrich                           | Cat# 172012                        |
| Penicillin-Streptomycin solution                              | FUJIFILM Wako Pure Chemical Corporation | Cat# 168-23191                     |
| 2-mercaptoethanol   | FUJIFILM Wako Pure Chemical Corporation | Cat# 135-14352; CAS No.60-24-2     |
| Phytohemagglutinin  | FUJIFILM Wako Pure Chemical Corporation | Cat# 161-15251; CAS No.9008-97-3   |
| <b>Critical commercial assays</b>                             |   |                                    |
| Mouse ANGPTL3 Assay Kit                                       | Immuno-Biological Laboratories          | Cat# 27410                         |
| Mouse ANGPTL8 Assay Kit                                       | MyBioSource, Inc                        | Cat# MBS456830                     |
| LabAssay Triglyceride   | FUJIFILM Wako Pure Chemical Corporation | Cat# 290-63701                     |
| LabAssay NEFA   | FUJIFILM Wako Pure Chemical Corporation | Cat# 290-63601                     |
| Lipid Extraction Kit  | Cell Biolabs, Inc.                      | Cat# STA-612                       |
| Lipid Quantification Kit (Fluorometric)                       | Cell Biolabs, Inc.                      | Cat# STA-617                       |
| PrimeScript RT reagent Kit                                    | Takara Bio Inc.                         | Cat# RR037B                        |
| SYBER Premix Ex TaqII   | Takara Bio Inc.                         | Cat# RR041A                        |
| Cell Counting Kit-8   | DOJINDO                                 | Cat# CK04                          |
| Mouse IFN- $\gamma$ Quantikine ELISA Kit                      | R&D Systems                             | Cat# MIF00                         |
| Mouse IL-2 Quantikine ELISA Kit                               | R&D Systems                             | Cat# M2000B                        |
| Mouse IL-4 Quantikine ELISA Kit                               | R&D Systems                             | Cat# M4000B                        |
| Mouse IL-10 Quantikine ELISA Kit                              | R&D Systems                             | Cat# M1000B                        |
| <b>Experimental models: Organisms/strains</b>                 |   |                                    |
| Mouse: B6.Cg- <i>Lep<sup>ob</sup>/J</i>                       | Charles River Laboratories              | RRID:IMSR_JAX:000632               |
| Mouse: B6.KOR/StmSlc- <i>ApoE<sup>shl</sup></i>               | Japan SLC                               | MGI Cat# 3716940; RRID:MGI:3716940 |
| Mouse: C57BL/6J   | Charles River Laboratories              | RRID:IMSR_JAX:000664               |
| <b>Software and algorithms</b>                                |   |                                    |
| GraphPad Prism (version 8.4.3)                                | GraphPad Software Inc.                  | RRID:SCR_002798                    |

(Continued on next page)

**Continued**

| Reagent or resource           | Source     | Identifier      |
|-------------------------------|------------|-----------------|
| Photoshop 2021 (version 22.5) | Adobe Inc. | RRID:SCR_014199 |
| STATA MP (version 15.0)       | StataCorp. | RRID:SCR_012763 |
| <b>Oligonucleotides</b>       |            |                 |
| Primers for realtime PCR      | This paper | Table S2        |

**RESOURCE AVAILABILITY**

**Lead contact**

Further information and requests for resources and reagents should be directed to and will be fulfilled by the lead contact, Yuichi Oike ([oike@gpo.kumamoto-u.ac.jp](mailto:oike@gpo.kumamoto-u.ac.jp)).

**Materials availability**

This study did not generate new unique reagents.

**Data and code availability**

All data generated from the study are included in the manuscript or in the supplemental information in the form of figures and tables. Data analysis methods are described in the section [statistical analysis](#).

**METHOD DETAILS**

**Vaccine design and synthesis**

We designed 3 candidate peptides: epitope1 (E1) corresponding to a region of the ANGPTL3 N-terminal sequence [17-25 amino acids (aa)]; E2 corresponding to a region of the C-terminal (416-425 aa); and E3 corresponding to a region of the LPL inhibitory domain (32-41 aa) ([Figure 1A](#); [Table S1](#)).<sup>13,19,20</sup> After synthesis, the N-terminal of each peptide was conjugated to KLH and synthetic peptides were purified by reverse-phase high performance liquid chromatography (HPLC) (> 98% purity) (Peptide Institute, Osaka, Japan). Peptide solutions were mixed with an equal volume of complete/incomplete Freund's adjuvant (FUJIFILM Wako Pure Chemical Corporation, Osaka, Japan) before immunization.

**Animal studies and immunization**

Animal experiments were approved by the Ethical Committee for Animal Experiments of the Kumamoto University, Graduate School of Medical Sciences.

**Obese-induced dyslipidemia mouse model**

Eight-week-old male B6.Cg-*Lep<sup>ob</sup>/J* (*ob/ob*) mice were purchased from Charles River Laboratories (Yokohama, Japan) and bred in conditions of 24°C, 12 hour light-dark cycles, and free access to normal chow and water. Mice were divided into 4 groups and intradermally immunized with 100 µg of KLH-conjugated ANGPTL3 peptide vaccines (E1-E3) or an equal quantity of KLH mixed with an equal volume of Freund's adjuvant as a control (n = 7-12 per group). Mice received identical immunizations at 2nd and 4th weeks after the first immunization. After 6 weeks, 10 µL of mouse serum was collected from the tail vein and then mice that had been fasted for 15 hours were sacrificed to collect liver and spleen tissues for analysis.

**Severe familial hypercholesterolemia (FH) mouse model**

The severe FH mouse model was established via loss of ApoE function. Six-week-old male B6.KOR/StmSlc-*ApoE<sup>shl</sup>* mice were purchased from Japan SLC Inc. (Hamamatsu, Japan). Starting at 8 weeks of age, mice were fed a 1.0% high cholesterol diet (FEED ONE, Yokohama, Japan), and intradermally immunized with 100 µg KLH-conjugated E3 peptide vaccine or an equal quantity of KLH control (n = 7-12 per group). Mice were comparably immunized at 2 and 4 weeks after the first immunization. At 6 weeks after the first immunization, blood samples were collected, and at 22 weeks, mice were fasted 15 hours and then sacrificed to evaluate atherosclerosis progression and circulating lipids.

**Evaluation of ANGPTL3 vaccine durability**

Eight-week-old male C57BL/6J wild-type mice were purchased from Charles River Laboratories (Yokohama, Japan) and bred as described above. Mice (n = 7-12) were intradermally immunized with 100 µg KLH-conjugated E3 peptide, followed by identical immunizations 2 and 4 weeks later. Controls were injected with KLH in Freund's adjuvant following the same protocol. To

evaluate vaccine durability, blood samples from mice in non-fasting conditions were collected from the tail vein at 6, 20, and 30 weeks after the first immunization, and antibody titers and non-fasting TG levels were assessed as described below.

### Evaluation of anti-ANGPTL3 antibody titers in immunized mice

Antibody titers were evaluated as described.<sup>35</sup> In brief, ELISA plates (MaxiSorp Nunc; Thermo Fisher Scientific, Waltham, Massachusetts) were coated with 5 mg/mL candidate ANGPTL3 peptides in carbonate buffer overnight at 4°C. Peptides were conjugated to BSA carrier protein (Peptide Institute). After blocking with PBS containing 5% skim milk, sera were diluted with a range from 100 to 312,500-fold in blocking buffer. After overnight incubation at 4°C and subsequent washing, plates were incubated with horseradish peroxidase (HRP)-conjugated antibodies specific for mouse IgG (GE Healthcare, Chicago, Illinois) for 3 h at room temperature. After washing with PBS, the color was developed using the peroxidase chromogenic substrate 3,3'-5,5'-tetramethyl benzidine (Sigma-Aldrich, St. Louis, Missouri), and the reaction was halted with 0.5 N sulfuric acid. Absorbance at 450 nm was monitored with a microplate reader (iMark, Bio-Rad, Hercules, California). The half-maximal antibody titer was determined according to the highest value in the dilution range of each sample.

### Western blot analysis

Recombinant mouse ANGPTL3 protein (R&D Systems, Minneapolis, Minnesota) and the BSA-conjugated E1-E3 epitopes were separated by SDS/PAGE and blotted onto PVDF membranes (Merck Millipore, Burlington, Massachusetts). After blocking with PBS containing 5% skim milk, membranes were incubated with immunized sera 1,000-fold diluted with Can Get Signal Solution 1 (TOYOBO, Osaka, Japan) or with anti-BSA antibody (Abcam Cat# ab79827, RRID: AB\_1603068; Abcam, Cambridge, United Kingdom) diluted 1,000-fold with the same solution. After washing and incubation with HRP-conjugated antibodies specific for mouse IgG (GE Healthcare), chemiluminescence signals were detected using an imaging system (Lilber, Marne-la-Vallée, France).

### Real-time polymerase chain reaction analysis

Total RNA was extracted using TRIzol reagent (Thermo Fisher Scientific) based on the manufacturer's protocol. Briefly, DNase-treated RNA was reverse-transcribed using a Prime Script RT reagent Kit (Takara Bio Inc, Shiga, Japan). Quantitative real-time PCR was performed using SYBER Premix Ex TaqII (Takara Bio Inc.). Relative transcript abundance was normalized to that of 18S rRNA levels of mice. Primer sequences are shown in [Table S2](#).

### Blood chemistry

Blood TG levels in non-fasting conditions and FFA levels in fasting conditions were measured by LabAssay kit (FUJIFILM Wako Pure Chemical Corporation) according to the manufacturer's protocol. Blood ALT levels at sacrifice were measured by SRL (Tokyo, Japan) and fasting lipid profile measurements by Skylight Biotech (Akita, Japan).

### Measurement of liver TG

Lipids in liver were extracted using a Lipid Extraction Kit (Cell Biolabs, Inc., San Diego, California) and then solubilized in 100  $\mu$ L methanol/chloroform mixture. TG were quantified using the Lipid Quantification Kit (Fluorometric) (Cell Biolabs, Inc.), according to the manufacturer's protocol. Measured TG values were normalized to the weight of liver used for extraction.

### Histological analysis

Paraffin-embedded liver tissue was sliced into 4  $\mu$ m sections and subjected to Hematoxylin-Eosin or Azan-Mallory staining. NAS [non-alcoholic fatty liver disease (NAFLD) activity score]<sup>21</sup> was used to assess NAFLD status. The degree of fibrosis was assessed based on the percentage of blue positivity in Azan-Mallory-stained sections. All imaging analysis was performed using a BZ-X 710 microscope (Keyence, Osaka, Japan).

### Evaluation of atherosclerosis progression

Aortas were collected from E3-vaccinated B6.KOR/StmSlc-Apoe<sup>shl</sup> mice and from KLH-treated controls and lipid-rich plaques were stained with Oil red O. Using Photoshop 2021 (version 22.5) (Adobe Inc., San Jose, California), the extent of plaque lesions was calculated as the percentage of the Oil red O-stained area relative to the entire area of the aorta.

### T cell proliferation assay

T cell proliferation was assessed as described.<sup>35</sup> In brief, spleens of euthanized mice were collected and minced, and splenocytes including T cells ( $10^6$  cells per well) were cultured in RPMI medium 1640 (FUJIFILM Wako Pure Chemical Corporation) containing 10% FBS (Sigma-Aldrich), 1% penicillin-streptomycin solution (FUJIFILM Wako Pure Chemical Corporation) and 50  $\mu$ M 2-mercaptoethanol (FUJIFILM Wako Pure Chemical Corporation), with supplementation with E3 peptide, KLH, or phytohemagglutinin (PHA) (FUJIFILM Wako Pure Chemical Corporation) at concentrations of 10  $\mu$ g/ml. After a 48 hr incubation at 37°C with 5% CO<sub>2</sub>, 10  $\mu$ L of the Cell Counting Kit-8 solution (DOJINDO, Kumamoto, Japan) was added to each well and incubated 4 hours. Splenocyte proliferation was assessed using a microplate reader at 450 nm. Concentrations of IFN- $\gamma$ , IL-2, IL-4 and IL-10 in supernatants were also measured using an ELISA kit (R&D systems), according to the manufacturer's instruction.

### Measurement of serum ANGPTL3 and ANGPTL8 levels

Serum ANGPTL3 protein levels were measured using a mouse ANGPTL3 ELISA kit (Immuno-Biological Laboratories, Gunma, Japan). Serum ANGPTL8 protein levels were measured using a mouse ANGPTL8 ELISA kit (MyBioSource, Inc., San Diego, California).

### Statistical analysis

Normality of continuous variables was evaluated by the Kolmogorov-Smirnov test. If the distribution was normal, data was expressed as means  $\pm$  SEM. Comparisons between two groups were made using Student's *t* test. In comparisons between three or more groups, one-way ANOVA with Dunnett's tests was employed. If the distribution was not normal, data was expressed as the median  $\pm$  interquartile range (IQR), and comparisons between two groups were made using the Mann-Whitney U test. The Kruskal-Wallis test with Dunn's test was performed in comparisons between three or more groups. A mixed effect model was applied to repeated-measures data using week effects, vaccine effects and interaction of both as explanatory variables. In this model, ID of individual mice was set as a random intercept. A likelihood ratio test was performed to evaluate statistical significance of the interaction.  $p < 0.05$  was considered statistically significant. Analyses were performed using GraphPad PRISM version 8.4.3 (GraphPad Software, Inc., La Jolla, California), and STATA MP 15.0 software (StataCorp., College Station, Texas).

**Cell Reports Medicine, Volume 2**

**Supplemental information**

**Vaccine targeting ANGPTL3 ameliorates dyslipidemia  
and associated diseases in mouse models of obese  
dyslipidemia and familial hypercholesterolemia**

**Hiroataka Fukami, Jun Morinaga, Hironori Nakagami, Hiroki Hayashi, Yusuke Okadome, Eiji Matsunaga, Tsuyoshi Kadomatsu, Haruki Horiguchi, Michio Sato, Taichi Sugizaki, Takashige Kuwabara, Keishi Miyata, Masashi Mukoyama, Ryuichi Morishita, and Yuichi Oike**



1 **Supplementary information**

2

3 Vaccine targeting ANGPTL3 ameliorates dyslipidemia and associated diseases in mouse models of obese  
4 dyslipidemia and familial hypercholesterolemia

5

6

7 Hiroataka Fukami, Jun Morinaga, Hironori Nakagami, Hiroki Hayashi, Yusuke Okadome, Eiji Matsunaga,  
8 Tsuyoshi Kadomatsu, Haruki Horiguchi, Michio Sato, Taichi Sugizaki, Takashige Kuwabara, Keishi  
9 Miyata, Masashi Mukoyama, Ryuichi Morishita, Yuichi Oike

10

11

1 **Supplementary tables**

2

3

4

5

6

7

8

9

10

| Peptide | Amino acid sequence                      |
|---------|--|
| E1      | <sup>17</sup> SRVDPDLSS <sup>25</sup>    |
| E2      | <sup>416</sup> KYNKPRTKSR <sup>425</sup> |
| E3      | <sup>32</sup> EPKSRFAMLD <sup>41</sup>   |

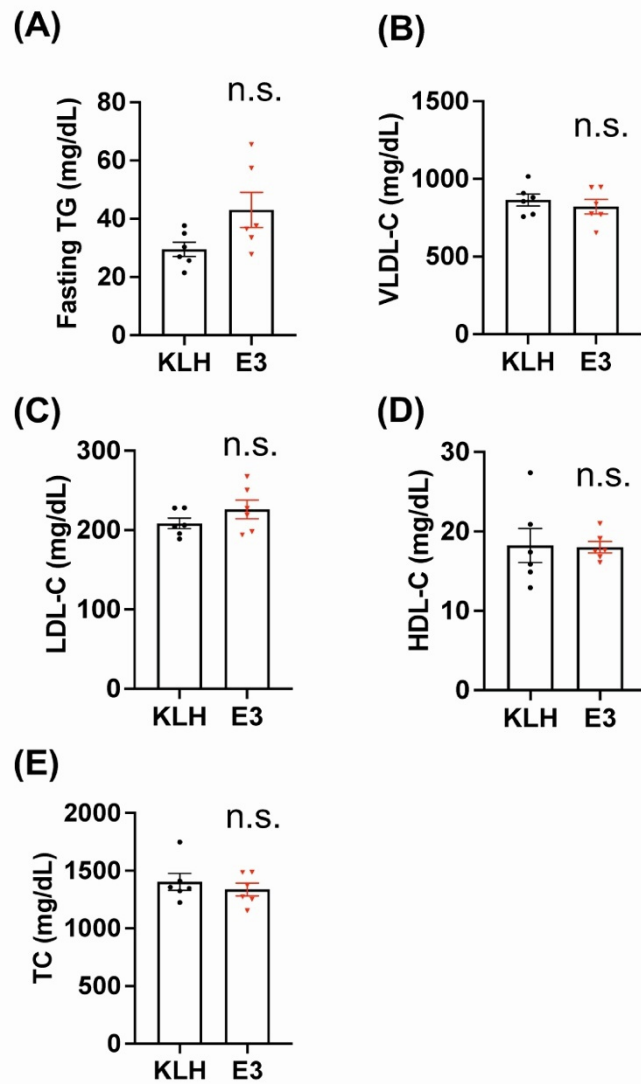
Table S1. Amino acid sequences of peptides E1–E3. Related to Figure 1.

| Gene           | Forward (5'-3')           | Reverse (5'-3')            |
|----------------|---------------------------|----------------------------|
| <i>Rps18</i>   | TTCTGGCCAACGGTCTAGACAAC   | CCAGTGGTCTTGGTGTGCTGA      |
| <i>Angptl3</i> | GATTTGCTATGTTGGATGATGTCAA | CTTATGGACAAAATCTTTAAGTCCA  |
| <i>Acc1</i>    | ACAGTGGAGCTAGAATTGGAC     | ACTTCCCGACCAAGGACTTTG      |
| <i>Fasn</i>    | AGCACTGCCTTCGGTTCAGTC     | AAGAGCTGTGGAGGCCACTTG      |
| <i>Il-6</i>    | CCACTTCACAAGTCGGAGGCTTA   | GCAAGTGCATCATCGTTGTTTCATAC |
| <i>Tnf</i>     | AAGCCTGTAGCCACGTCGTA      | GGCACCACTAGTTGGTTGTCTTTG   |
| <i>Colla1</i>  | GAGCGGAGAGTACTGGATCGA     | CTGACCTGTCTCCATGTTGCA      |
| <i>Col3a1</i>  | CAACCAGTGCAAGTGACCAA      | GCACCATTGAGACATTTTGAAG     |

1

2 Table S2. Sequences of primers used for quantitative RT-PCR of mouse genes. Related to Oligonucleotides  
3 in Star Methods.

4



1  
2 Figure S1. Evaluation of long-term efficacy of the E3 vaccine against dyslipidemia in severe familial  
3 hypercholesterolemia model mice. (A-E) Blood samples from *ApoE<sup>shl</sup>* mice fed a high cholesterol  
4 diet were analyzed 22 weeks after the first immunization (n=6 per group). Levels of (A) fasting TG, (B)  
5 fasting VLDL-C, (C) fasting LDL-C, (D) fasting HDL-C, and (E) fasting TC in circulation. Results are  
6 expressed as mean  $\pm$  SEM. n.s. not significant. Related to Figure 5.